



Alcohol lean burn in heavy duty engines: Achieving 25 bar IMEP with high efficiency in spark ignited operation

Mahendar, Senthil Krishnan; Larsson, Tara; Erlandsson, Anders Christiansen

Published in:
International Journal of Engine Research

Link to article, DOI:
[10.1177/1468087420972897](https://doi.org/10.1177/1468087420972897)

Publication date:
2021

Document Version
Peer reviewed version

[Link back to DTU Orbit](#)

Citation (APA):
Mahendar, S. K., Larsson, T., & Erlandsson, A. C. (2021). Alcohol lean burn in heavy duty engines: Achieving 25 bar IMEP with high efficiency in spark ignited operation. *International Journal of Engine Research*, 22(11), 3313–3324. <https://doi.org/10.1177/1468087420972897>

General rights

Copyright and moral rights for the publications made accessible in the public portal are retained by the authors and/or other copyright owners and it is a condition of accessing publications that users recognise and abide by the legal requirements associated with these rights.

- Users may download and print one copy of any publication from the public portal for the purpose of private study or research.
- You may not further distribute the material or use it for any profit-making activity or commercial gain
- You may freely distribute the URL identifying the publication in the public portal

If you believe that this document breaches copyright please contact us providing details, and we will remove access to the work immediately and investigate your claim.

Alcohol lean burn in heavy duty engines: Achieving 25 bar IMEP with high efficiency in spark ignited operation

Senthil Krishnan Mahendar¹ , Tara Larsson¹ and Anders Christiansen Erlandsson^{1,2}

International J of Engine Research

1–12

© IMechE 2020



Article reuse guidelines:

sagepub.com/journals-permissions

DOI: 10.1177/1468087420972897

journals.sagepub.com/home/jer



Abstract

Knock is the most crucial limitation in attaining the peak load required at high efficiency in heavy duty (HD) spark ignited (SI) engines. Renewable fuels such as ethanol and methanol have high resistance to autoignition and can help overcome this limitation. To reduce knock and improve efficiency further, dilution can be used to add specific heat capacity and reduce combustion temperature. This work studied diluted combustion and knock characteristics of gasoline, ethanol, and methanol on a HD SI single cylinder engine for a wide load range. Ethanol and methanol displayed excellent knock resistance which allowed a peak gross IMEP of 25.1 and 26.8 bar respectively, compared to gasoline which only reached 8.3 bar at $\lambda = 1.4$ with a compression ratio of 13. Over 18% increase in gross IMEP was possible for gasoline and ethanol when increasing air excess ratio from 1 to 1.4. Methanol achieved the target gross IMEP at $\lambda = 1$ and required no spark retard at $\lambda = 1.6$. A peak indicated efficiency above 48% was recorded for ethanol and methanol at $\lambda = 1.6$ and gross IMEP of approximately 21 bar. At part loads, stable operation was possible until $\lambda = 1.8$ for all fuels. Increase in intake temperature showed a marginal improvement in stability but no increase in lean limit. The concept shows promise as diluted combustion of ethanol and methanol reduced knock and achieved diesel baseline load. With optimization, there is potential to improve efficiency further and possible cost savings compared to commercial diesel engines.

Keywords

Ethanol, methanol, excess air dilution, knock, heavy duty

Date received: 2 July 2020; accepted: 20 October 2020

Introduction

Road freight transport is expected to surpass private transport as the largest greenhouse gas emitter within the transportation sector by 2030.¹ To decarbonize the freight transport sector, renewable fuels are viewed as an important strategy.² There are possible biomass based renewable fuel production methods, such as gasification, that generate methanol, ethanol and other higher alcohols. Additionally, as a simple molecule, methanol can also be produced as an “electro-fuel,” potentially even from atmospheric carbon dioxide.^{1,3,4} These varied production pathways make alcohols a promising low-carbon future fuel for the transport sector. Currently, world production of renewable fuels constitute around 75% ethanol and 25% bio-diesel and the share of alcohols could increase in the future.

Alcohols, such as ethanol and methanol, have a high octane number (listed in Table 1) and cannot be used directly in conventional diesel combustion process without ignition improvers, increased compression ratio or an ignition source.^{5–8} Another way to introduce alcohols in HD engines is to utilize premixed ethanol or methanol with a diesel pilot ignition source. With premixed alcohols, studies have reported control over a

¹KTH Royal Institute of Technology Industrial Engineering and Management, Stockholm, Sweden

²Technical University of Denmark – DTU, Denmark

Corresponding author:

Senthil Krishnan Mahendar, Department of Machine Design, KTH Royal Institute of Technology Industrial Engineering and Management, Brinellvägen 83, Stockholm, SE-100 44, Sweden.

Email: mahendar@kth.se

Table 1. Fuel properties.^{12–14}

Property	Gasoline	Methanol	Ethanol
Composition	–	CH ₃ -OH	C ₂ H ₅ -OH
Lower heating value, MJ/kg	42.7	19.9	26.8
Heat of vaporization, MJ/kg	0.18	1.17	0.93
Stoichiometric air fuel ratio	14.7 : 1	6.45 : 1	9 : 1
Research octane number (RON)	90–100	109	109
Peak laminar flame speed, cm/s at 1 bar and $\lambda = 1$	48.3 @ 358K	52.2 @ 343K	49.6 @ 343K

wide load range and low emissions but a high pressure rise rate limits the premixed alcohol fraction that can be used, especially at high loads.^{9–11} Additionally, dual fuel engines require two fuel handling systems and have to retain the high pressure diesel injection systems thereby increasing capital costs. Instead, high octane ethanol and methanol can be used relatively easily in spark ignited (SI) engines.

HD SI engines are an attractive option due to their low noise and lower system cost. If operated stoichiometric, a simple three-way catalyst and control would suffice as after-treatment. However, HD SI engines are limited in operating range and efficiency by engine knock.

Knock is defined as the auto-ignition of the unburned fuel-air mixture (end gas) ahead of the flame front. As the flame propagates, the pressure and temperature of the end gas increase which could result in end gas auto-ignition, rapid heat release, undesirable noise and potential engine damage due to high heat transfer. In HD SI engines, knock will be worsened compared to light duty engines since a larger bore diameter causes a longer residence time for the end gas at high temperature and pressure. Moreover, a higher boost pressure is necessary to achieve the required engine load, which would further exacerbate knock.

Apart from conventional knock discussed earlier, there is potential for super-knock especially if the engine is direct injected. Super-knock phenomenon and mitigation strategies has been discussed in detail by previous works.^{15–19} In addition, studies^{20–22} have reported preignition potential of various fuels and blends. Despite the high resistance to auto-ignition of ethanol, the longer injection duration and wall wetting increases pre-ignition occurrences that could lead to super-knock.^{22,23} Although not in the scope of this study, super-knock is important to consider in HD SI engines as load and speed ranges are similar to downsized and boosted spark ignition engines

To mitigate knock, increase load range and efficiency in HD SI engines, low carbon alcohols exhibit suitable properties as shown in Table 1. Apart from the high research octane number (RON), ethanol and methanol have high heat of vaporization (HOV) which reduces temperature. Since the lower heating value (LHV) of alcohols are lower, more fuel injection is required and as a result, significantly higher

temperature reduction due to evaporation can be achieved by ethanol and methanol over gasoline.

In addition to higher RON and HOV, alcohols' resistance to low temperature heat release (LTHR) further improves knock reduction. Gasoline end gas ignition delay shows a negative temperature coefficient (NTC) in the transition from low to high temperature chemistry. As the end gas temperature increases over 750K, the change in ignition delay decreases and is highly relevant in the knock performance of boosted and spark retard operation.^{15,17,24–26} With increase in boost pressure over 1.5 bar-a, LTHR becomes a limitation in SI gasoline engines.²⁷ Unlike gasoline, ethanol and methanol do not exhibit an NTC region and has a much longer ignition delay time in the low and medium temperature regimes, thereby allowing increased boosting compared gasoline.²⁰

Though alcohols favor knock reduction and increased specific torque compared to gasoline, it is not clear if the diesel engine IMEP can be achieved in HD SI engines. On a HD single cylinder engine, Ottosson and Zioris²⁸ used port fuel injected E85 to achieve 17 bar IMEP (knock limited) at 39% indicated efficiency at stoichiometric operation. The lower efficiency reported was due to spark retard to mitigate knock at increased boost pressures. Using a similar engine, Björnestrand²⁹ studied methanol direct injection at lean conditions and observed over 45% indicated efficiency at a load of 8 bar IMEP.

Results from light duty engines fueled with alcohols show an improvement in both BMEP and efficiency.^{30–33} Notably, Brusstar et al.³⁴ and Brusstar and Gray³⁵ used ethanol and methanol on a SI converted light duty and medium duty diesel engine. Without a peak pressure or boost limitation, they achieved 18 bar and 20 bar BMEP using E85 and M85 respectively.³⁵

To increase engine load further, mixture dilution can be used. Through exhaust gas recirculation (EGR) or excess air addition, the specific heat capacity of the unburned fuel air mixture can be increased, which reduces combustion temperature.³⁶ This reduction in temperature aids knock reduction and also offers higher efficiency due to lower heat loss. Apart from the temperature effect, there is also a reduction in chemical reactivity leading to higher end gas autoignition delay times for leaner mixtures.^{37,38} With both chemical and temperature advantages, studies^{39–42} have shown

reduced knock tendency with EGR and more favorable phasing for gasoline fueled engines. Similar to EGR, excess air dilution also reduces knock and is the focus of this study.

The effect of dilution on ethanol and methanol fueled engines and knocking behavior is captured by few studies. Gukelberger et al.⁴³ and Kaiser et al.⁴⁴ observed a marginal efficiency improvement for E85 with EGR but not as much as gasoline since E85 was already close to optimal phasing. In these cases, the potential for improvement was limited by hardware used, that is, boost pressure or peak pressure limitation. For instance, Brusstar and Gray³⁵ report significantly higher loads if boost and peak pressures are not limited while using over 20% EGR.

The challenge to increasing dilution is combustion instability. Mixed results for stability are reported comparing gasoline and ethanol^{31,45–48} and are elaborated in a previous work.⁴⁹ Ethanol, with a higher HOV, results in lower temperature at spark timing than gasoline and hence potentially lower stability. On the other hand, ethanol is more volatile and has a marginally higher laminar flame speed which should reduce instability. The effect of temperature seemed to be a key factor as shown by Moxey et al.,⁴⁸ where increased residual gas content reduced instability in ethanol and increased instability for iso-octane. Further investigation into the effect of increasing intake temperature on dilution limit of ethanol and methanol fuel is required. Increased intake temperature could aid in increasing lean operation and efficiency over a wider map, especially in part load operation to minimize throttling loss.

To match diesel engine operating load, an IMEP of over 25 bar is required from the HD SI engine. This load has to be achieved with relatively high efficiency as high load operation is prevalent in HD engine operation for acceleration and gradients. Theoretically, the highest efficiency and IMEP can be realized at high dilution where the engine is limited by both knock and instability.

This study experimentally investigates the influence of ethanol and methanol fuel in combination with excess air dilution on engine knock. In addition, the effect of increasing intake temperature on combustion instability with diluted operation of these high HOV fuels were investigated. Engine performance has been evaluated at higher pressure and temperature conditions than previous studies, which will be a proof of concept and aid in validating simulation models at more relevant operating conditions for HD engine application.

Experimental setup

The experiment was performed on a HD single cylinder engine rig available at KTH Royal Institute of Technology. The engine is based on the Scania D12 and was adapted with port fuel injectors and a central

Table 2. Test engine specification.

Bore	127 mm
Stroke	154 mm
Connecting rod length	255 mm
Compression ratio	13
Engine speed	1200 rpm
Number of cylinders	1
Mixture formation	PFI
Piston bowl diameter	105 mm
Intake valve close (IVC)	−154 deg aTDC
Exhaust valve open (EVO)	145 deg aTDC

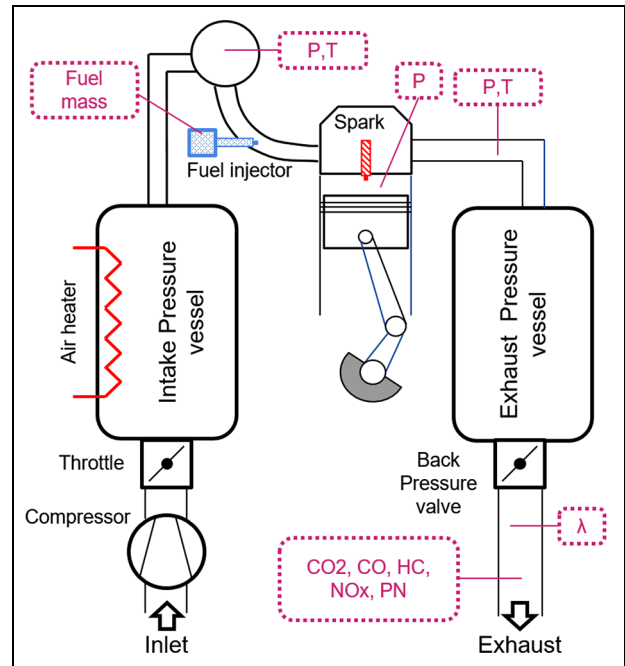


Figure 1. Experimental setup – single cylinder engine rig.

spark plug. A custom piston was used to reduce compression ratio (CR) to 13 from the diesel baseline CR of 17.1. A bathtub style geometry was used to minimize potential hot spots and is shown as “baseline” in a previous publication.⁵⁰ A CR of 13 is fairly higher than boosted LD gasoline and was chosen to improve efficiency for part load ethanol and methanol. The stock diesel cylinder head and intake ports were used which produces swirl. The engine specifications are listed in Table 2 and the test set up is shown in Figure 1.

The test cell is equipped with an independent external compressor to simulate boosted operation. A back pressure valve was used to maintain back pressure equal to the intake pressure at boosted operation so that residual level in-cylinder will be comparable to a full engine. The intake temperature was maintained constant at 30°C for the full load cases. The oil and coolant conditioning systems also retained a constant temperature of 90°C throughout the tests. Exhaust temperature was limited to 750°C and intake boost pressure was limited to 2.5 bar in our setup.

The fuel system was constructed with two high flow Bosch EV14 injectors placed approximately 30 cm upstream of the valve at each intake port. A fuel injection pressure of 5 bar relative to intake pressure was used through an inline pump and a mechanical fuel pressure regulator. For all cases, fuel was injected during the valve open period with start of injection at intake valve open (IVO). As a low LHV fuel, methanol required a long injection time of up to 180 CAD but was completed before IVC. A Bosch wide-band oxygen sensor and ETAS lambda meter were used to maintain set point excess air ratio within ± 0.025 . A Denso 5717 spark plug mounted in the center of the cylinder head was used with the stock Scania EURO 5 gas engine's ignition coil. In a swirl combustion chamber, the central spark position was chosen to minimize mean velocity at the spark plug. A lower mean velocity should theoretically produce lower chance of spark blow out, have lower cycle variation and higher lean limit for a given ignition energy.⁵¹ The coil charging time was maintained constant for all fuels and operating points. The engine was controlled using an in-house software and constant spark timing was used without any knock control. Since spark timing was manually set, knock limited spark advance (KLSA) was defined as spark advance when maximum amplitude of pressure oscillation (MAPO) of the high pass filtered pressure signal reached over 1 bar for 1 to 3% of the sampled cycles.

Data acquisition

Cylinder pressure at 0.1 CAD resolution was sampled using a flush mounted AVL GU21D pressure sensor and a Kistler 5011 charge amplifier. A fuel container was used and consumption from the container was measured using a Sartorius MW1P1-150FE-L industrial scale. Raw emissions were measured through a Horiba MEXA 7100 DEGR gas analyzer. Gross indicated mean effective pressure, $IMEP_g$, is used as an indicator of engine load (equation (1)). The indicated efficiency, η_{ind} , is calculated based on $IMEP_g$ and measured fuel flow shown in equation (3). The combustion instability limit was defined as 5% COV of $IMEP_g$ (equation (2)).

$$IMEP_g = \frac{1}{V_{sw}} \int_{V_{BDC, compression}}^{V_{BDC, expansion}} P dV \quad (1)$$

$$COV = \frac{\sigma_{IMEP_g}}{IMEP_g} \quad (2)$$

$$\eta_{ind} = \frac{0.5 n IMEP_g V_{sw}}{\dot{m}_{fuel} Q_{LHV,f}} \quad (3)$$

$$AROHR = \frac{\gamma}{\gamma - 1} P \frac{dV}{dCAD} + \frac{1}{\gamma - 1} V \frac{dP}{dCAD} \quad (4)$$

$$\eta_{comb} = 1 - \frac{\sum \frac{M_i}{M_p} x_i (1 - x_{H_2O}) Q_{LHV,i}}{\frac{1}{1 + A/F} Q_{LHV,f}} \quad (5)$$

Where, P = ensemble averaged and pegged in-cylinder pressure signal (Pa); V = calculated cylinder volume (m^3); V_{sw} = cylinder swept volume (m^3); \dot{m}_{fuel} = fuel mass flow measured (kg/s); n = engine speed (s^{-1}); $Q_{LHV,f}$ = fuel lower heating value (J/kg); γ = specific heat ratio; M_i = molar mass of HC and CO emission (g/mol); M_p = Molar mass of products (g/mol); x_i = mol fraction of HC and CO emissions; x_{H_2O} = mol fraction of water in exhaust; $Q_{LHV,i}$ = heating value of HC and CO emissions (J/kg) and A/F = air fuel ratio

Apparent rate of heat release (AROHR) calculated using Eqn. 4, is used to estimate burn duration, CA1075 and anchor angle, CA50. CA1075 is the crank angle required to burn 10% to 75% of unburned mixture and is used to describe the burn rate in this study. CA50 is the point where 50% of fuel-air mass has burned and is used to describe combustion phasing. Flame development time, CA10, is the crank angle degree (CAD) required to achieve 10% burned fraction from spark timing. The in-cylinder mass is calculated based on measured fuel flow and lambda. The in-cylinder temperature is calculated using the ideal gas law and a 7-coefficient NASA polynomial is used to calculate the specific heat ratio, γ .⁵² From an estimate at a comparable load, 60K drop in cylinder temperature was observed for ethanol compared to gasoline before combustion. This is in line with the study by Kasseris and Heywood⁵³ while also considering the higher injection quantity of ethanol for the same load point. Methanol, on the other hand, saw only a 30K drop compared to gasoline and was most likely due to wall wetting. From the temperature and γ estimates, burned and unburned mixture fractions are linearly fit based on a burn duration calculation with constant $\gamma = 1.3$ as an intermediate iteration before calculating cylinder specific heat ratio.⁵⁴

The hydrocarbon emissions reported by the flame ionization detector (FID) in the exhaust gas analyzer are corrected for alcohol fuels to account for the weaker response in oxygenated fuels. A response factor of 0.7 and 0.4 is used for ethanol and methanol respectively.^{55,56}

Test methodology

The test plan was designed to evaluate knock limited operation of gasoline, ethanol and methanol at increasing levels of excess air dilution at 1200 rpm. The knock limited $IMEP_g$ and η_{ind} were obtained by performing boost pressure sweeps at constant excess air ratios from 1 to 1.8 in steps of 0.2. Spark timing at each operating point was advanced to optimal timing for maximum brake torque (MBT) or KLSA depending on the knock level.

To evaluate part load performance for ethanol and methanol, 8.5 bar $IMEP_g$ was used as a target and the same lambda steps from 1 to 1.8 was evaluated. Additionally, the effect of intake temperature on part

load combustion and stability was evaluated at 30, 45, and 60°C for ethanol and methanol.

Results

The effect of excess air dilution in combustion and knock limits of gasoline, ethanol and methanol are presented. To match diesel engine loads, a target of 25 bar IMEP_g was chosen. Performance and emissions in full load and part load are discussed.

Full load— $\lambda = 1.4$

Within the limitations of the set up used, peak IMEP_g (shown in Figure 2) was achieved with an excess air ratio of 1.4 for all fuels. Gasoline was knock limited at 8.3 bar IMEP_g. Boosting and further retardation in combustion phasing was not possible due to high COV. Ethanol achieved the target IMEP_g of 25 bar with a similarly retarded phasing and COV. Methanol surpassed the target by reaching 26.8 bar IMEP_g with minimal spark retard.

Both ethanol and methanol reached the boost pressure limit in the experimental setup used. Due to lower knock, methanol CA50 was phased earlier and recorded 46.8% indicated efficiency at full load. The peak pressure was well within diesel limits for all fuels. At full load, methanol showed 134 bar-a peak pressure due to its earlier combustion phasing as shown in Figure 2. The better phasing also corresponded to faster heat release (Figure 2(f)) when compared to similarly phased gasoline and ethanol.

Full load – Effect of dilution

The peak load achieved at each dilution level and the performance and emissions for those points are shown in Figures 3 to 5. With increasing dilution, specific heat capacity is added thus reducing temperature and knock. This is seen from $\lambda = 1$ to 1.4, for gasoline and ethanol in Figure 3(a), where over 18% increase in IMEP_g was seen. Notably, methanol exceeded the target 25 bar IMEP_g without dilution. Increasing dilution from 1 to 1.6, methanol combustion phasing at peak load could be advanced progressively until MBT as shown in Figure 3(c). Combustion duration, CA1075 shown in 3 d, of methanol was lower than the other fuels because CA50 on average was closer to TDC where in-cylinder turbulence is higher.

At $\lambda = 1.6$, gasoline had over 5% COV above CA50 of 20 deg aTDC and hence could not be boosted any further. No more increase in IMEP_g was possible for the alcohols since they reached the intake pressure limit of the set up. Ethanol was still knock limited whereas methanol could run at MBT.

With increasing dilution, efficiency also increased as a function of reducing heat transfer and favorable combustion phasing as seen in Figure 4(a). Compared to gasoline, ethanol and methanol showed about 5 and

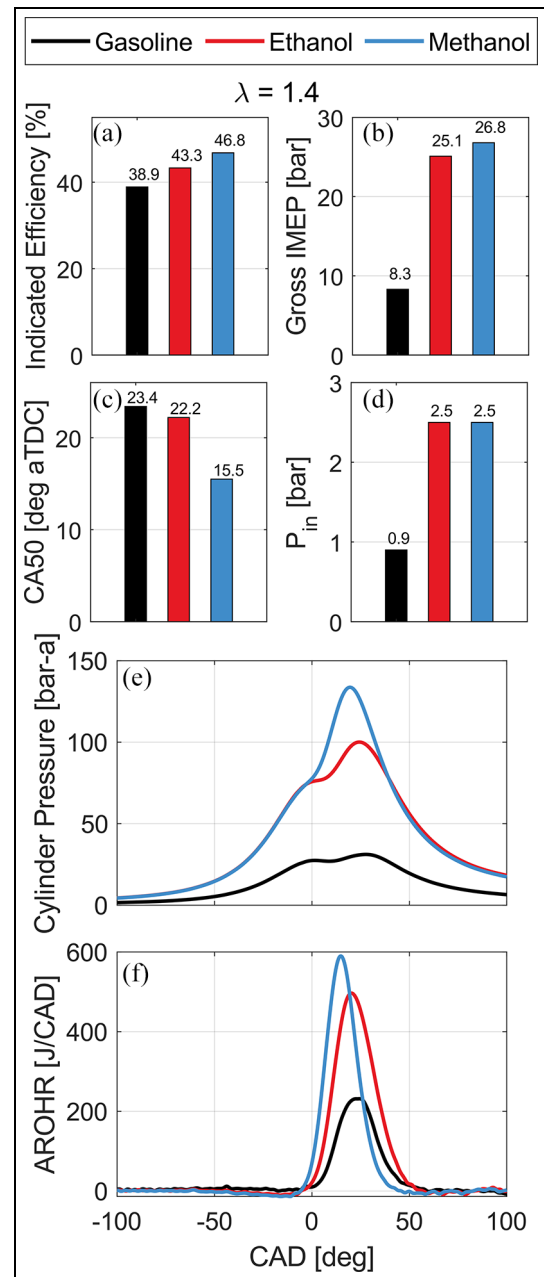


Figure 2. Peak IMEP at $\lambda = 1.4$ (a) indicated efficiency (b) gross IMEP (c) combustion phasing, CA50 (d) intake pressure (e) mean cylinder pressure, and (f) mean apparent rate of heat release for the test fuels.

8% point improvement in efficiency respectively and much higher IMEP_g. Over 5% point increase in indicated efficiency was possible at $\lambda = 1.8$ compared to stoichiometric operation for all fuels at full load. Even though gasoline achieved only a third of the load, the exhaust temperature was only 50°C lower as shown in Figure 4(d), due to the high spark retard and low heat of vaporization. Methanol, with a higher heat of vaporization, gave lower exhaust temperature than ethanol for 6 bar higher IMEP_g at $\lambda = 1$. Figure 4(b) shows that peak pressure of the ensemble averaged pressure signal was maximum at $\lambda = 1.6$ for the alcohol fuels.

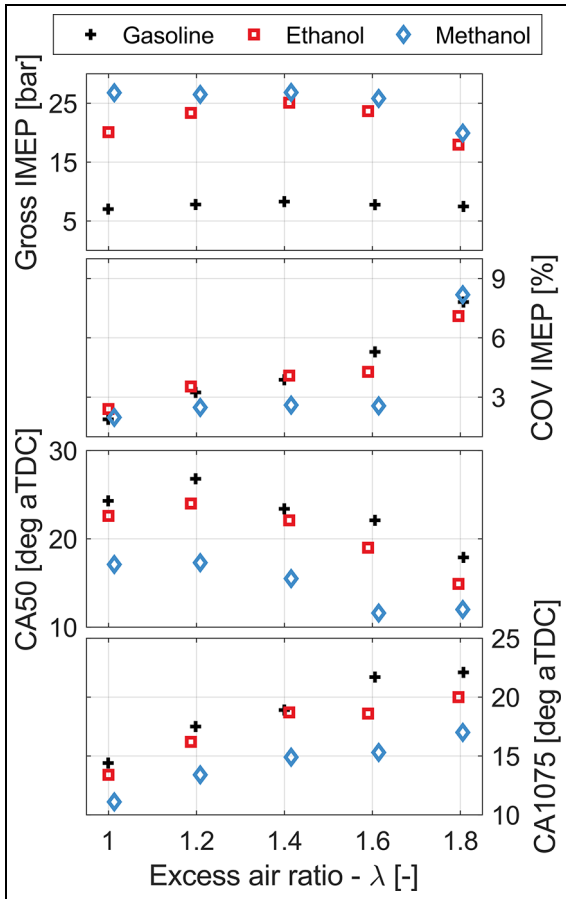


Figure 3. Peak load points – (a) $IMEP_g$ (b) stability, COV of $IMEP_g$ (c) combustion phasing, CA50, and (d) combustion duration, CA1075.

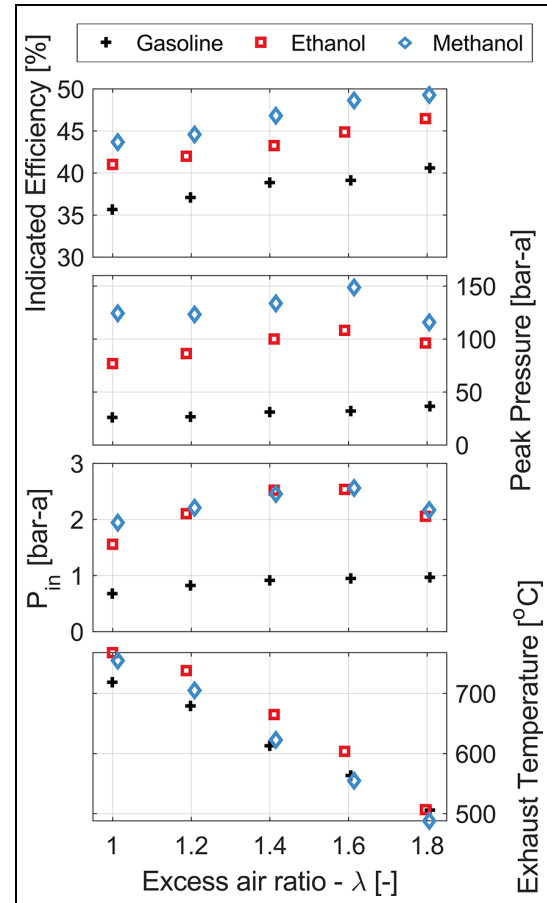


Figure 4. Peak load points—(a) indicated efficiency (b) peak pressure (c) intake pressure, and (d) exhaust temperature.

At $\lambda = 1.8$, high COV reduced the load possible, hence a lower peak pressure is seen.

The corrected HC emissions show a similar trend for all fuels in Figure 5(a) with respect to excess air ratio. Gasoline had the lowest load and in-cylinder temperature, thereby produced the highest specific HC. With a large HOV and high injection quantity, methanol showed a sharp HC increase from $\lambda = 1.2$ to $\lambda = 1.8$. CO emissions, in Figure 5(b), are higher for alcohol fuels at $\lambda = 1.2$ and $\lambda = 1.4$ compared to gasoline. However, this is at much higher pressure-temperature conditions and could be due to increased CO_2 dissociation. Interestingly, specific NOx emission shows no advantage for the high HOV alcohol fuels as seen in Figure 5(c), but reduced with increasing dilution.

Knock limit: Load increase

Figure 6 presents the effect of increasing IMEP to knock limited CA50 for gasoline, ethanol and methanol at $\lambda = 1, 1.4, \text{ and } 1.6$. Gasoline requires retardation in phasing already at 5.4 bar $IMEP_g$ when operated stoichiometric. With increased dilution, spark retard is required at 7 bar $IMEP_g$. A CR of 13 was chosen to improve efficiency in ethanol and methanol fuels. For

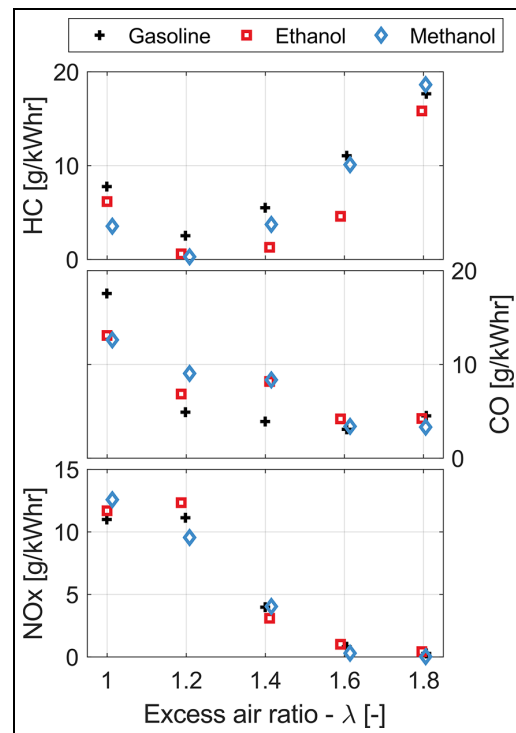


Figure 5. Peak load points—emissions (a) corrected unburned hydrocarbons (b) carbon monoxide, and (c) oxides of nitrogen.

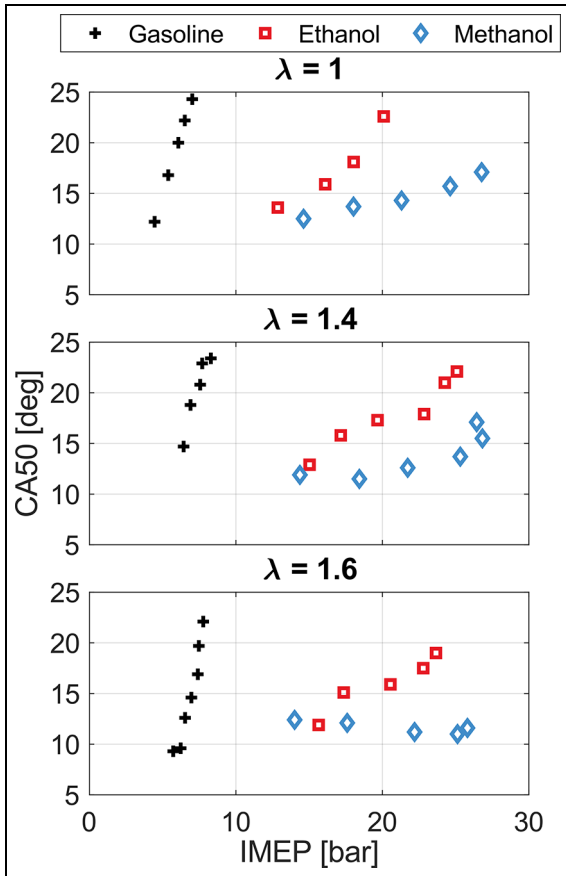


Figure 6. Load sweep—knock limited CA50 for (a) $\lambda = 1$ (b) $\lambda = 1.4$, and (c) $\lambda = 1.6$.

gasoline, it was significantly high and hindered boosting. The boost pressure required to achieve the corresponding IMEP is shown in Figure 7. Gasoline could not be boosted at all and was knock limited with WOT operation at this CR. Ethanol and methanol both reached the boost pressure limitation of the test setup. At higher loads, methanol required lower boosting to achieve the same IMEP due to better combustion phasing as shown in Figure 6. At $\lambda = 1.8$, boost pressure could not be increased beyond 2.1 bar-a due to excessive COV.

In the case of ethanol (Figure 6), retardation for knock was required only above 16 bar IMEP_g at $\lambda = 1$ and the range of MBT operation increases to 17.5 bar IMEP_g with dilution. Methanol required spark retard only over 21 bar IMEP_g at $\lambda = 1$, over 25 bar IMEP_g at $\lambda = 1.4$ and required no spark retard at $\lambda = 1.6$.

The indicated efficiency curves, shown in Figure 8, follow the CA50 trend especially for gasoline. Notably, ethanol and methanol showed much lower efficiency penalty for spark retard than gasoline. This may be due to the lower in-cylinder temperature and heat loss for the alcohol fuels. At $\lambda = 1.6$, ethanol and methanol show an indicated efficiency over 48% at approximately 21 bar IMEP_g. At higher loads, with retardation in combustion phasing, ethanol efficiency drops while

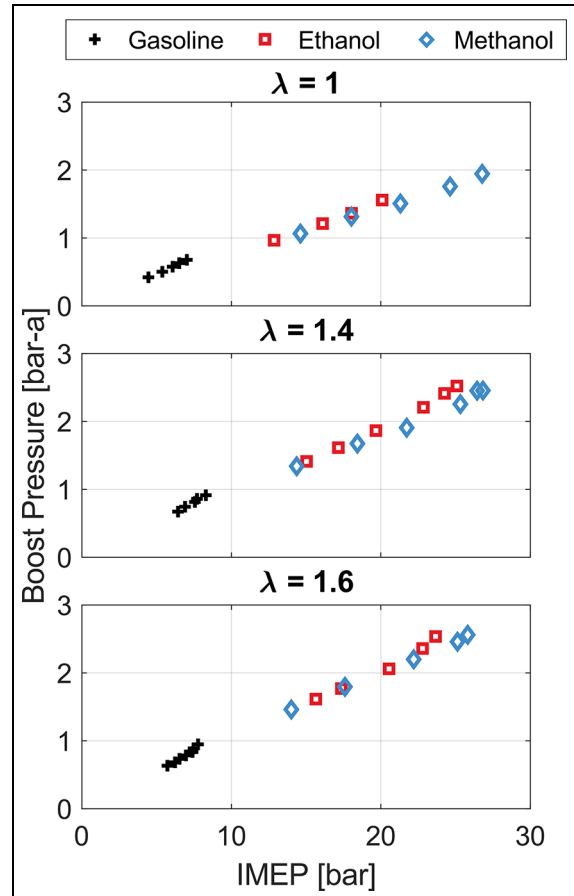


Figure 7. Load sweep—intake pressure for (a) $\lambda = 1$ (b) $\lambda = 1.4$, and (c) $\lambda = 1.6$.

methanol shows similar indicated efficiency until target peak load.

At full load, burn duration (CA1075) showed sensitivity to dilution but could not be compared at similar phasing between the fuels, as seen in Figure 3(c) and (d). Typically, spark retard caused the flame to propagate post TDC where the turbulence level in-cylinder is falling thereby increasing burn duration. It was only possible to achieve a third of the load with gasoline, hence results are at different pressure-temperature conditions in the full load case while comparing fuels. To better study the effect of fuel and dilution on combustion characteristics, knock limited gasoline is compared with part load ethanol and methanol in the subsequent section.

Part load: Effect of dilution

In this section, part load ethanol and methanol combustion characteristics is compared to knock limited gasoline at the tested lambda points. The load for alcohols was maintained at 8.5 bar IMEP_g (close to truck highway cruise load). The data includes spark sweeps at constant fuelling for the alcohol fuels whereas gasoline points include load changes as well. The results from all the points tested (about 5 points per fuel at each dilution level), are averaged and shown in Figures 9 and 10.

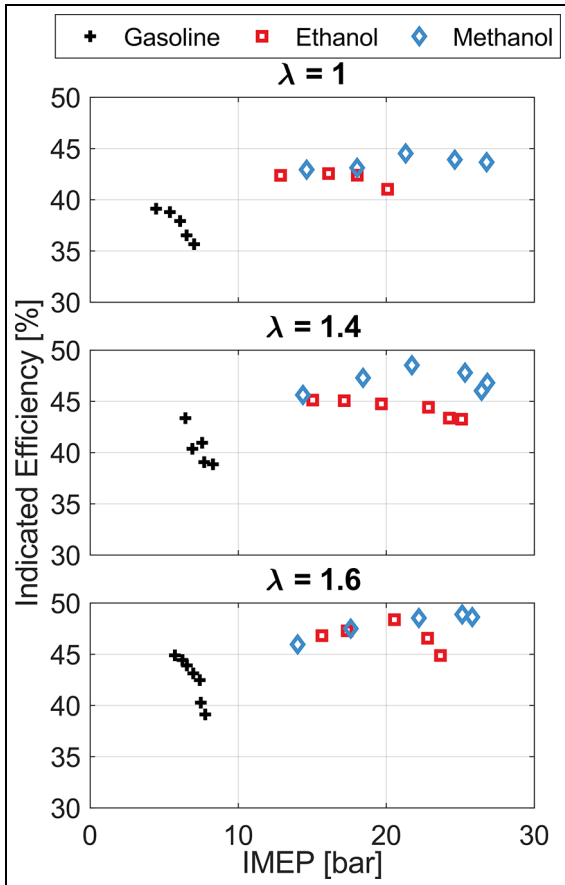


Figure 8. Load sweep—indicated efficiency for (a) $\lambda = 1$ (b) $\lambda = 1.4$, and (c) $\lambda = 1.6$.

Figure 9 compares the mean combustion characteristics of the fuels where the error bars indicate twice standard deviation for the points tested. The large spread in CA50 shown in Figure 9(c) is due to spark sweeps. Overall, there is no significant difference between fuels for CA1075 seen in Figure 9(a). The mean CA50 for gasoline was higher at lower excess air dilution which causes higher CA1075 since combustion occurs at lower turbulence post TDC. Ethanol and methanol showed similar burn duration until $\lambda = 1.8$ where ethanol started to deviate. The flame development time, CA010 shown in Figure 9(b), is also strongly dependent on excess air ratio. Methanol has a significantly higher laminar flame speed compared to gasoline and ethanol hence recorded the lowest flame development time despite having the highest HOV. Gasoline and ethanol showed similar flame development time. At $\lambda = 1.8$, ethanol showed higher flame development time even with statistically significant outliers removed indicating that ethanol has the lowest lean limit of the fuels tested.

Comparing emissions shown in Figure 10 to the full load case previously shown in Figure 5, the trend is inverted for HC emissions in part load conditions. With a higher HOV, flame quenching occurs earlier and methanol produced the highest corrected HC emissions. Gasoline and ethanol are on a similar level at

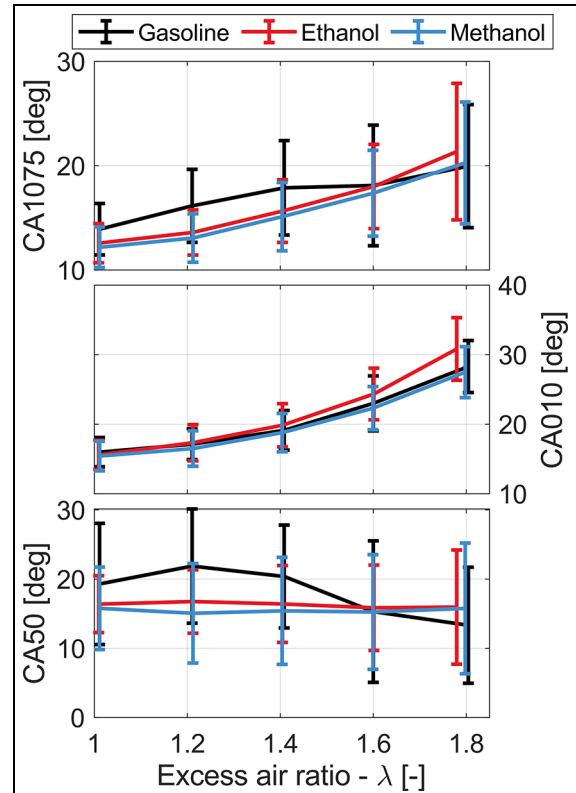


Figure 9. Part load spark sweep—mean value with error bars indicating twice standard deviation for (a) burn duration CA1075, (b) flame development time CA010, and (c) combustion phasing CA50.

most excess air conditions. At comparable load, CO and NO_x emissions are similar for all fuels.

At the same load and CA50 shown in Figure 11, ethanol and methanol showed similar indicated efficiency over the range of dilution levels tested. Indicated efficiency increased from 43% to 45.5% when excess air ratio was increased from $\lambda = 1$ to $\lambda = 1.6$ at 8.5 bar IMEP_g. However, methanol did have about 1% point lower combustion efficiency (calculated using equation (5) and shown in Figure 11(d)) than ethanol due to the higher HC emissions.

Part load: Effect of increasing intake temperature

To test the sensitivity of temperature at spark advance to combustion stability in high HOV fuels, the air supply was heated in steps of 15°C: 30°C (baseline), 45°C and 60°C. The combustion phasing was maintained within 2 deg of each other and an IMEP_g of 8.5 bar was maintained at all excess air dilution levels. The test was not performed with gasoline due to risk of pre-ignition.

With increasing temperature, there was a reduction in flame development time, CA010, seen in Figure 12(b) and (d). Increasing temperature from 30°C to 60°C, CA010 reduction ranges from 0.7 deg at $\lambda = 1.2$ to 2.1 deg at $\lambda = 1.8$. There was no significant difference in

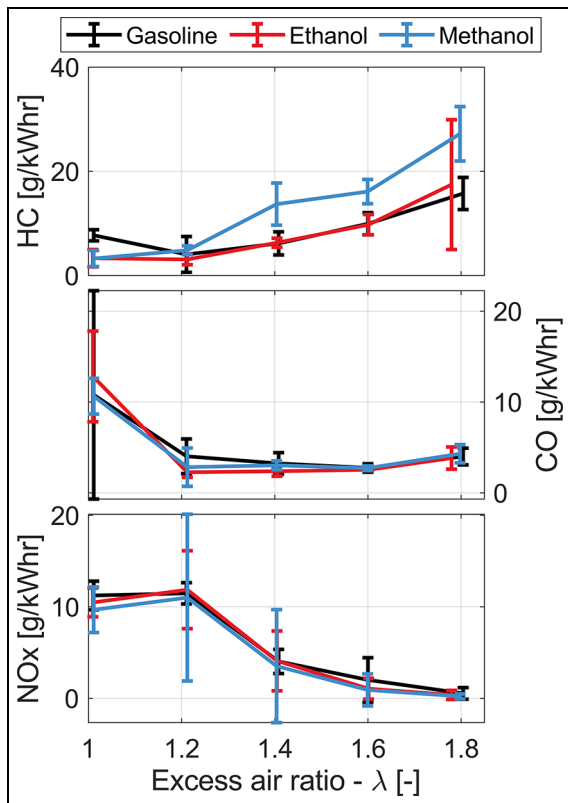


Figure 10. Part load spark sweep—mean value with error bars indicating twice standard deviation for (a) corrected unburned hydrocarbon, (b) carbon monoxide, and (c) oxides of nitrogen.

magnitude of reduction between the fuels. However, it should be noted that methanol CA10 was lower on average compared to ethanol at all excess air ratios and temperatures.

Methanol showed lower COV on average due to its lower flame development time. Similar to CA10 reduction, the same relative drop in COV due with increasing temperature was seen for both ethanol and methanol, as shown in Figure 12. In spite of the increase in temperature, lean limit could not be increased in both fuels. At $\lambda = 1.8$, regardless of reduction in CA10, high COV was observed and no clear trend with increasing intake temperature was seen.

Discussion

In a single cylinder heavy duty SI engine, knock was effectively limited by ethanol and methanol through high RON, high HOV and lack of a NTC region. Similar to Pischinger et al.,²⁰ our results show that ethanol boost pressure can be increased by about 60% over gasoline at $\lambda = 1.4$. Excess air dilution up to $\lambda = 1.8$ was possible with a production ignition coil and spark plug. $\lambda = 2$ was briefly tested but combustion stability was well over 10% with excessive misfires for all fuels. Lean limit could potentially be extended beyond $\lambda = 1.8$ with a higher energy ignition system. In this study, boost pressure was limited to 2.5 bar-a

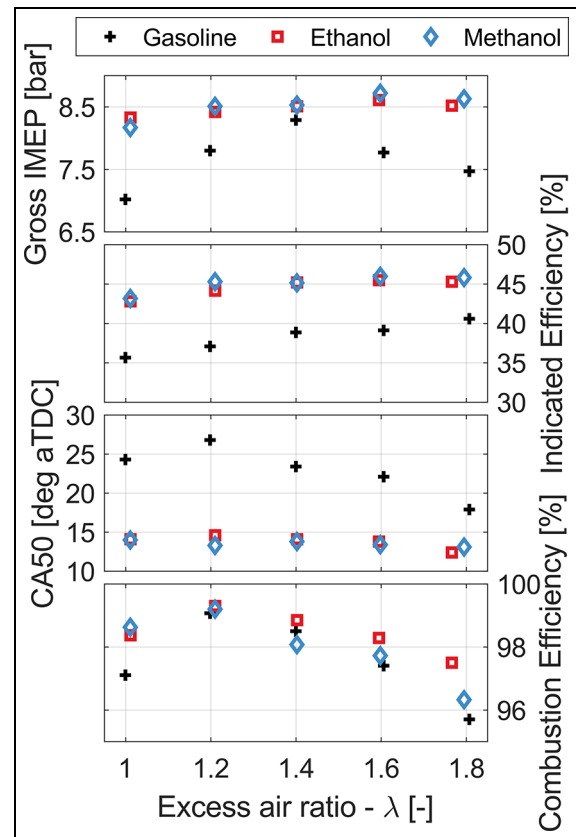


Figure 11. Part load comparison at similar phasing (a) $IMEP_g$, (b) indicated efficiency, (c) phasing, CA50, and (d) combustion efficiency.

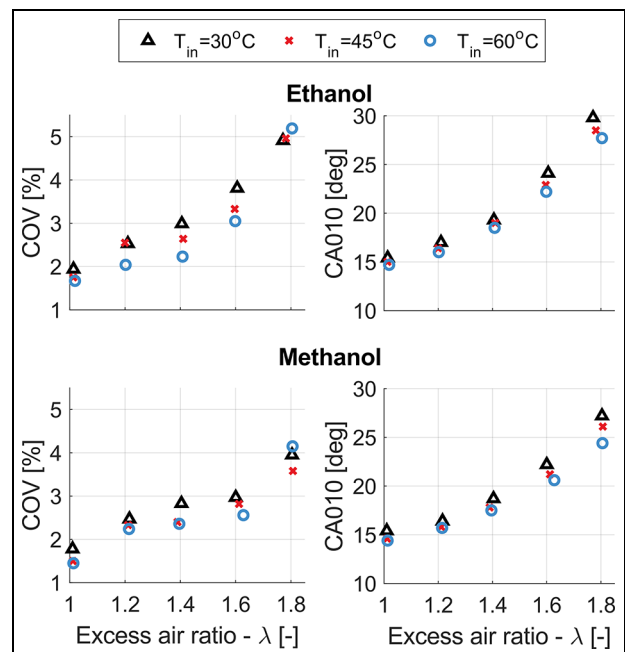


Figure 12. Intake temperature effect on (a) ethanol COV of $IMEP_g$ (b) ethanol CA010 (c) methanol COV of $IMEP_g$ and (d) methanol CA010.

and was a constraint in achieving 25 bar $IMEP_g$ at excess air ratio $\lambda = 1.6$.

The boost pressure and peak pressure requirements were within operating limits of diesel engines and minimum changes are required to convert diesel to SI combustion. However, one drawback to the study is that intake temperature was maintained at 30°C even at high boost pressures. This may not be feasible in operation and more tests are required to evaluate the influence of increased temperature on knock and load limitation. Also, intake and exhaust pressures were maintained equal in this study to ensure knock was assessed at a similar residual level as a full engine. With turbocharging, there is possibility that a positive or negative pressure differential might arise and its effect on knock performance has to be assessed. If back pressure is higher than boost pressure, residual gas level and in-cylinder temperature would likely be higher which would lead to a lower knock limited IMEP. If boost pressure is higher than back pressure, potential scavenging loss has to be minimized in port injected engines.

At part load $\lambda = 1.6$, about 45.5% indicated efficiency was seen for both ethanol and methanol. This increases to over 48% at about 21 bar IMEP_g for both fuels. Above 21 bar IMEP_g methanol has similar indicated efficiency but ethanol efficiency is limited by knock. To improve efficiency further in HD SI engines, some methods have been compiled and discussed in a previous publication.⁴⁹ EGR could potentially offer higher dilution level compared to excess air^{36,41} thereby improving efficiency. Using EGR, dilution can be achieved at global stoichiometric air fuel ratio and a three way catalyst can be used thereby simplifying the after treatment architecture.

In the experiment, the engine used had swirl ports which does not significantly contribute to turbulence increase and in addition, causes heat loss during the expansion stroke. Swirl in LD diesel engines have been attributed to cause 0.5% point reduction in indicated efficiency⁵⁷ hence it is worth investigating further in HD SI engines. To improve the benefit of dilution, combustion speed can be increased further through increased turbulence. LD engines use tumble ports and pentroof combustion chambers where the bulk velocity breaks down into turbulence close to TDC and aids in improving combustion speed. However, this calls for a complete re-design of the cylinder head and will be justified if the production volume is significant.

A simpler change may be using piston shapes to improve squish and increase turbulence close to TDC. The potential improvement offered by higher squish pistons were tested through a previous simulation study⁵⁰ compared to the piston used in this experimental study. With increase in combustion speed, the end gas could be consumed before the critical residence time for auto-ignition is reached. Moreover, increased flame speed could aid faster flame development and lower COV at elevated dilution.^{58,59}

With increase in dilution, exhaust temperature reduces which poses a challenge to maintain high after treatment efficiency. In this study, IMEP below 8 bar

was not tested and exhaust temperatures remained above the critical limit of 400°C for ethanol and methanol. With lower loads, after treatment efficiency may be a limitation in achieving high dilution and needs further investigation. Although exhaust enthalpy reduces with dilution, the enthalpy available until an excess air ratio of $\lambda = 1.4$ is similar to diesel engines and a comparable turbocharger setup would suffice. If higher dilution levels are required at full load, turbocharging would be a very critical design consideration. Moreover, the CR in a SI engine is a major limitation in improving efficiency. To increase efficiency, expansion ratio can be increased while maintaining compression ratio for knock through Miller valve timing.^{60,61} Since a higher boost pressure is needed to maintain the required air mass, diluted Miller operation places even more emphasis on the charging system. Further study is required to assess the demands of Miller timing diluted HD SI engines and the charging system architecture required.

Summary

- Knock limited 26.8 bar and 25.1 bar IMEP_g was demonstrated with methanol and ethanol respectively, on a port fuel injected heavy duty spark ignited engine at excess air dilution of $\lambda = 1.4$.
- Over 18% increase in IMEP_g was possible for gasoline and ethanol when excess air ratio was increased from stoichiometric to $\lambda = 1.4$. Corresponding indicated efficiencies increased by 2.2% point for ethanol and 3.2% point for gasoline.
- Methanol exceeded the target 25 bar IMEP_g even at stoichiometric operation. The knock limited CA50 could be advanced from 16 deg aTDC at $\lambda = 1$ to MBT at $\lambda = 1.6$ thereby showing a 2.8% point increase in indicated efficiency.
- Peak efficiency of over 48% was recorded for both ethanol and methanol at an excess air ratio of $\lambda = 1.6$ around 21 bar IMEP_g. Higher excess air ratios typically introduced high COV and lower combustion efficiency with the ignition set up used.
- With increased dilution at and above $\lambda = 1.6$, spark retard and boosting was not possible over CA50 of 20 deg aTDC for ethanol and gasoline due to high COV.
- Instability was generally high for $\lambda = 1.8$ for all fuels. Methanol had the least flame development time (CA010) of the fuels tested. Ethanol at $\lambda = 1.8$ showed significant increase in CA010 suggesting that it had the lowest lean limit of the fuels tested.
- At part load, with increase in intake temperature, a decrease in COV was observed for most excess air points but it did not help increase lean limit beyond $\lambda = 1.8$.

Acknowledgements

The authors would like to thank Magnus Bjurman (Volvo CE), Johan Engström (Volvo GTT) and Ludvig

Adlercreutz (industrial PhD student at KTH) for their support and feedback during this work.

Declaration of conflicting interests

The author(s) declared no potential conflicts of interest with respect to the research, authorship, and/or publication of this article.

Funding

The author(s) disclosed receipt of the following financial support for the research, authorship, and/or publication of this article: The Competence Center for Gas Exchange (CCGEx), and its partners are acknowledged for the financing for this work.

ORCID iD

Senthil Krishnan Mahendar  <https://orcid.org/0000-0002-0705-2677>

References

- IEA. Energy technology perspectives 2017. Catalysing energy technology transformations. Technical report, 2017.
- Reitz RD, Ogawa H, Payri R, et al. IJER editorial: the future of the internal combustion engine. *Int J Engine Res* 2020; 21(1): 3–10.
- Larsson T, Stenlaas O and Erlandsson A. Future fuels for DISI engines: a review on oxygenated, liquid biofuels. SAE technical paper 2019-01-0036, 2019.
- Verhelst S, Turner JW, Sileghem L and Vancoillie J. Methanol as a fuel for internal combustion engines. *Prog Energy Combust Sci* 2019; 70: 43–88.
- Velazquez S, Melo EH, Moreira JR, Apolinario SM and Coelho ST. Ethanol usage in urban public transportation - presentation of results. SAE technical paper 2010-36-0130, 2010.
- Tuner M. Review and benchmarking of alternative fuels in conventional and advanced engine concepts with emphasis on efficiency, CO₂, and regulated emissions. SAE technical paper 2016-01-0882, 2016.
- Saccullo M, Benham T and Denbratt I. Dual fuel methanol and diesel direct injection HD single cylinder engine tests. SAE technical paper 2018-01-0259, 2018.
- Giramondi N, Jäger A, Mahendar SK and Erlandsson A. Combustion characteristics, performance and NO_x emissions of a heavy-duty ethanol-diesel direct injection engine. SAE technical paper 2020-01-2077, 2020.
- Sarjovaara T, Alantie J and Larmi M. Ethanol dual-fuel combustion concept on heavy duty engine. *Energy* 2013; 63: 76–85.
- Pedrozo VB, May I, Guan W and Zhao H. High efficiency ethanol-diesel dual-fuel combustion: a comparison against conventional diesel combustion from low to full engine load. *Fuel* 2018; 230: 440–451.
- Guan W, Wang X, Zhao H and Liu H. Exploring the high load potential of diesel-methanol dual-fuel operation with Miller cycle, exhaust gas recirculation, and intake air cooling on a heavy-duty diesel engine. *Int J Engine Res*. Epub ahead of print June 2020. DOI: 10.1177/1468087420926775.
- Owen K and Coley T. *Automotive fuels reference book*. 2nd ed. Warrendale, PA: Society of Automotive Engineers, 1995.
- Dirrenberger P, Glaude PA, Bounaceur R, et al. Laminar burning velocity of gasolines with addition of ethanol. *Fuel* 2014; 115: 162–169.
- Veloo PS, Wang YL, Egolfopoulos FN and Westbrook CK. A comparative experimental and computational study of methanol, ethanol, and n-butanol flames. *Combust Flame* 2010; 157(10): 1989–2004.
- Wang Z, Liu H and Reitz RD. Knocking combustion in spark-ignition engines. *Prog Energy Combust Sci* 2017; 61: 78–112.
- Kalghatgi G, Algunaibet I and Morganti K. On knock intensity and superknock in SI engines. *SAE Int J Engines* 2017; 10(3): 1051–1063.
- Kalghatgi G. Knock onset, knock intensity, superknock and preignition in spark ignition engines. *Int J Engine Res* 2017; 19: 7–20.
- Singh E, Hlaing P, Shi H and Dibble R. Effect of different fluids on injection strategies to suppress pre-ignition. SAE technical paper 2019-01-0257, 2019.
- Singh E and Dibble R. Mechanism triggering pre-ignition in a turbo-charged engine. SAE technical paper 2019-01-0255, 2019.
- Pischinger S, Günther M and Budak O. Abnormal combustion phenomena with different fuels in a spark ignition engine with direct fuel injection. *Combust Flame* 2017; 175: 123–137.
- Ottenwälder T, Burke U, Hoppe F, et al. Experimental and numerical study of abnormal combustion in direct injection spark ignition engines using conventional and alternative fuels. *Energy Fuels* 2019; 33: 5230–5242.
- Haenel P, Kleeberg H, de Bruijn R and Tomazic D. Influence of ethanol blends on low speed pre-ignition in turbo-charged, direct-injection gasoline engines. *SAE Int J Fuels Lubr* 2017; 10(1): 95–105.
- Singh E and Dibble R. Knock, auto-ignition and pre-ignition tendency of fuels for advanced combustion engines (FACE) with ethanol blends and similar RON. SAE technical paper 2020-01-0613, 2020.
- Pan J, Wei H, Shu G, Chen Z and Zhao P. The role of low temperature chemistry in combustion mode development under elevated pressures. *Combust Flame* 2016; 174: 179–193.
- Szybist JP and Splitter DA. Pressure and temperature effects on fuels with varying octane sensitivity at high load in SI engines. *Combust Flame* 2017; 177: 49–66.
- Lavoie G, Middleton R, Martz J, Makkapati S and Curtis E. Characteristic time analysis of SI knock with retarded combustion phasing in boosted engines. SAE technical paper 2017-01-0667, 2017.
- Szybist JP, Wagnon SW, Splitter D, Pitz W and Mehl M. The reduced effectiveness of EGR to mitigate knock at high loads in boosted SI engines. *SAE Int J Engines* 2017; 10(5): 2305–2318.
- Ottosson D and Zioris K. *Experimental comparison of DI and PFI in terms of emissions and efficiency running Ethanol-85*. Technical report, KTH, Machine Design (Dept.), 2014.
- Björnestrand L. *Efficiency and emission analysis of a methanol fuelled direct injection spark ignition heavy duty engine*. Technical report, Lund: Lund University, 2017.

30. Kasseris EP. *Knock limits in spark ignited direct injected engines using gasoline / ethanol blends*. PhD Thesis, Massachusetts Institute of Technology, Cambridge, 2011.
31. Warnberg J, Boehmer M and Denbratt I. Optimised neat ethanol engine with stratified combustion at part-load; particle emissions, efficiency and performance. SAE technical paper 2013-01-0254, 2013.
32. Szybist J, Foster M, Moore WR, Confer K, Youngquist A and Wagner R. Investigation of knock limited compression ratio of ethanol gasoline blends. SAE technical paper 2010-01-0619, 2010.
33. Sileghem L, Ickes A, Wallner T and Verhelst S. Experimental investigation of a DISI production engine fuelled with methanol, ethanol, butanol and ISO-stoichiometric alcohol blends. SAE technical paper 2015-01-0768, 2015.
34. Brusstar M, Stuhldreher M, Swain D and Pidgeon W. High efficiency and low emissions from a port-injected engine with neat alcohol fuels. SAE technical paper 2002-01-2743, 2002.
35. Brusstar M and Gray CL. High efficiency with future alcohol fuels in a stoichiometric medium duty spark ignition engine. SAE technical paper 2007-01-3993, 2007.
36. Grandin B and Ångström HE. Replacing fuel enrichment in a turbo charged SI engine: lean burn or cooled EGR. SAE technical paper 1999-01-3505, 1999.
37. Mittal G, Burke SM, Davies VA, Parajuli B, Metcalfe WK and Curran HJ. Autoignition of ethanol in a rapid compression machine. *Combust Flame* 2014; 161(5): 1164–1171.
38. Kumar K and Sung C. Autoignition of methanol: experiments and computations. *Int J Chem Kinet* 2011; 43(4): 175–184.
39. Alger T, Mangold B, Roberts C and Gingrich J. The interaction of fuel anti-knock index and cooled EGR on engine performance and efficiency. *SAE Int J Engines* 2012; 5(3): 1229–1241.
40. Alger T, Chauvet T and Dimitrova Z. Synergies between high EGR operation and GDI systems. *SAE Int J Engines* 2008; 1(1): 101–114.
41. Cairns A, Blaxill H and Irlam G. Exhaust gas recirculation for improved part and full load fuel economy in a turbocharged gasoline engine. SAE technical paper 2006-01-0047, 2006.
42. Hoepke B, Jannsen S, Kasseris E and Cheng W. EGR effects on boosted SI engine operation and knock integral correlation. *SAE Int J Engines* 2012; 5(2): 547–559.
43. Gukelberger R, Alger T, Mangold B, Boehler J and Eiden C. Effects of EGR dilution and fuels on spark plug temperatures in gasoline engines. SAE technical paper 2013-01-1632, 2013.
44. Kaiser M, Krueger U, Harris R and Cruff L. “Doing more with less” - the fuel economy benefits of cooled EGR on a direct injected spark ignited boosted engine. SAE technical paper 2010-01-0589, 2010.
45. Varde KS and Manoharan NK. Characterization of exhaust emissions in a SI engine using E85 and cooled EGR. SAE technical paper 2009-01-1952, 2009.
46. Moxey BG, Cairns A and Zhao H. A study of turbulent flame development with ethanol fuels in an optical spark ignition engine. SAE technical paper 2014-01-2622, 2014.
47. Sementa P, Maria Vaglieco B and Catapano F. Thermodynamic and optical characterizations of a high performance GDI engine operating in homogeneous and stratified charge mixture conditions fueled with gasoline and bio-ethanol. *Fuel* 2012; 96: 204–219.
48. Moxey B, Cairns A and Zhao H. A comparison of burning characteristics of iso-octane and ethanol fuels in an optical SI engine. *J KONES* 2013; 20. DOI: 10.13140/2.1.3722.5288.
49. Mahendar SK, Erlandsson A and Adlercreutz L. Challenges for spark ignition engines in heavy duty application: a review. SAE technical paper 2018-01-0907, 2018.
50. Mahendar SK, Giramondi N, Venkataraman V and Erlandsson AC. Numerical investigation of increasing turbulence through piston geometries on knock reduction in heavy duty spark ignition engines. SAE technical paper 2019-01-2302, 2019.
51. Heywood J. *Internal combustion engine fundamentals*. Heywood: McGraw-Hill, 1988.
52. Burcat A and Ruscic B. *Third millennium ideal gas and condensed phase thermochemical database for combustion with updates from active thermochemical tables*. Technical report, 2005. DOI: 10.2172/925269.
53. Kasseris E and Heywood J. Charge cooling effects on knock limits in SI di engines using gasoline/ethanol blends: part 1-quantifying charge cooling. SAE technical paper 2012-01-1275, 2012.
54. Tunestål P. Self-tuning gross heat release computation for internal combustion engines. *Control Eng Pract* 2009; 17(4): 518–524.
55. Wallner T. Correlation between speciated hydrocarbon emissions and flame ionization detector response for gasoline/alcohol blends. *J Eng Gas Turbine Power* 2011; 133(8): 082801.
56. Daniel R, Wang C, Xu H, Tian G and Richardson D. Dual-injection as a knock mitigation strategy using pure ethanol and methanol. *SAE Int J Fuels Lubr* 2012; 5(2): 772–784.
57. Broatch A, Martín J, García A, Blanco-Cavero D, Warey A and Domenech V. Application of a zero-dimensional model to assess the effect of swirl on indicated efficiency. *Int J Engine Res* 2019; 20(8–9): 837–848.
58. Berntsson AW, Josefsson G, Ekdahl R, Ogink R and Grandin B. The effect of tumble flow on efficiency for a direct injected turbocharged downsized gasoline engine. *SAE Int J Engines* 2011; 4(2): 2298–2311.
59. Takahashi D, Nakata K, Yoshihara Y, Ohta Y and Nishiura H. Combustion development to achieve engine thermal efficiency of 40 for hybrid vehicles. SAE technical paper 2015-01-1254, 2015.
60. Zhang FR, Okamoto K, Morimoto S and Shoji F. Methods of increasing the BMEP (power output) for natural gas spark ignition engines. SAE technical paper 981385, 1998.
61. Luisi S, Doria V, Stroppiana A, Millo F and Mirzaeian M. Experimental investigation on early and late intake valve closures for knock mitigation through miller cycle in a downsized turbocharged engine. SAE technical paper 2015-01-0760, 2015.